1 Radar Measurements

The radar scenario involves a transmitter and a receiver (usually at the same location) with one or two antennas, a target at range R, and a signal that travels the round-trip between the radar and the target. The target sometimes has a velocity relative to the radar, in which case the range rate $\dot{R}$ is also measurable (Fig. 1.1).

The transmitted signal is usually an electromagnetic signal (but an acoustic one is also a possibility). The signal can be described by a carrier sine wave at frequency f_c with modulation of one or more of its parameters—amplitude, phase, and frequency.

The changes observed in the returned signal can provide information about the target position and sometimes its character. In simple terms, the delay of the returned signal yields information on the range. The frequency shift (Doppler) yields information on the range rate (velocity). The antenna pointing direction yielding maximum return strength (or other criteria) provides the azimuth and elevation of the target relative to the radar. From the progress of some of these parameters with time, the target's trajectory can be estimated.

DELAY AND RANGE

In radar the relationship between the delay τ and the range R is given by

$$R = \tfrac{1}{2}\tau C_P \tag{1.1}$$

where C_P is the velocity of propagation. The factor of $\frac{1}{2}$ is the result of the round trip travel time. The propagation velocity is not exactly the speed of

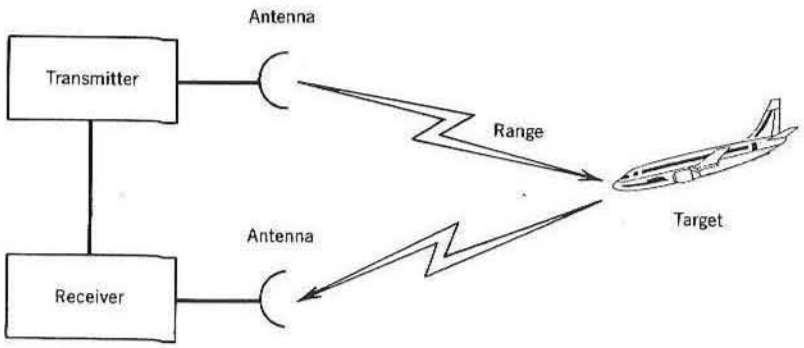

Figure 1.1 *A typical radar scene.*

light C ($C = 299.7925$ m/μs), because radar signals do not propagate in vacuum but in a real atmosphere. As we will see at the end of this chapter, they do not propagate in straight lines either. However, a good approximation, which we will generally use, is a straight-line propagation at a constant speed C.

DOPPLER SHIFT AND RANGE RATE

The Doppler frequency shift will be defined as the difference between the received frequency and the transmitted frequency. Thus

$$f_D = f_R - f_T \tag{1.2}$$

Neglecting second-order effects (relativistic, acceleration, etc.) the Doppler shift is related to the range rate $\dot{R}$ by

$$f_D = -\frac{2\dot{R}}{\lambda} \tag{1.3}$$

where the wavelength λ is given by

$$\lambda = \frac{C}{f_T} \tag{1.4}$$

The transmitted frequency of a signal is not a single value, since most signals have some bandwidth. For narrow-band signals replacing the transmitted frequency with the carrier frequency is sufficient, whereas for wide-band signals more complicated measures, involving Doppler broadening, are necessary. In our text we will usually assume, for a given target velocity, the same

Doppler shift for the entire signal bandwidth. A proof of (1.3) for a continuous wave (CW) signal is given in Insert 1A.

INSERT 1A Doppler Shift

Consider a transmitted signal whose voltage equation is

$$v_T(t) = \sin(2\pi f_T t + \phi_0) \tag{1A.1}$$

where ϕ_0 is the phase at $t = 0$. The signal is reflected from a moving point target whose range from the radar is given by

$$R(t) = R_0 + \dot{R}t \tag{1A.2}$$

where R_0 is the range at $t = 0$ and where it was assumed that the acceleration and higher range derivatives are equal to zero. The signal received back at the radar, neglecting attenuation, is the one transmitted τ seconds earlier—namely,

$$v_R(t) = v_T(t - \tau) \tag{1A.3}$$

or

$$v_R(t) = \sin[2\pi f_T(t - \tau) + \phi_0] \tag{1A.4}$$

where the delay is given by

$$\tau(t) = \frac{2R(t)}{C} \tag{1A.5}$$

Ignoring the change in range during the signal travel time, since usually $\dot{R} \ll C$, we can use the value of τ that existed at the time of receiving—namely, at t; hence

$$\tau = \frac{2(R_0 + \dot{R}t)}{C} \tag{1A.6}$$

Substituting (1A.6) in (1A.4) yields

$$v_R(t) = \sin\left(2\pi f_T t - 2\pi f_T \frac{2\dot{R}}{C} t - 4\pi f_T \frac{R_0}{C} + \phi_0\right). \tag{1A.7}$$

All the terms in the argument that multiply $2\pi t$ are frequencies. Hence we define

$$f_D = -f_T \frac{2\dot{R}}{C} = -\frac{2\dot{R}}{\lambda} \tag{1A.8}$$

and rewrite (1A.7) as

$$v_R(t) = \sin\left(2\pi(f_T + f_D)t - 4\pi f_T \frac{R_0}{C} + \phi_0\right) \tag{1A.9}$$

which leads to a received frequency of

$$f_R = f_T + f_D \tag{1A.10}$$

THE RADAR EQUATION

The target's range, velocity, and bearing can be measured very accurately when the return signal-to-noise ratio (SNR) is very high. They can be detected within a certain range and velocity windows, at somewhat lower SNR. The radar equation is our source of information on the expected return signal and SNR.

Assume that a radar transmits a pulse with power P_T, and seeks the return from a target at a range R (Fig. 1.2). If the radar transmitting antenna had an isotropic radiation pattern, then it would have spread the power with spherical symmetry, and the power flux per unit area at range R would have been

$$\text{Power density} = \frac{P_T}{4\pi R^2}$$

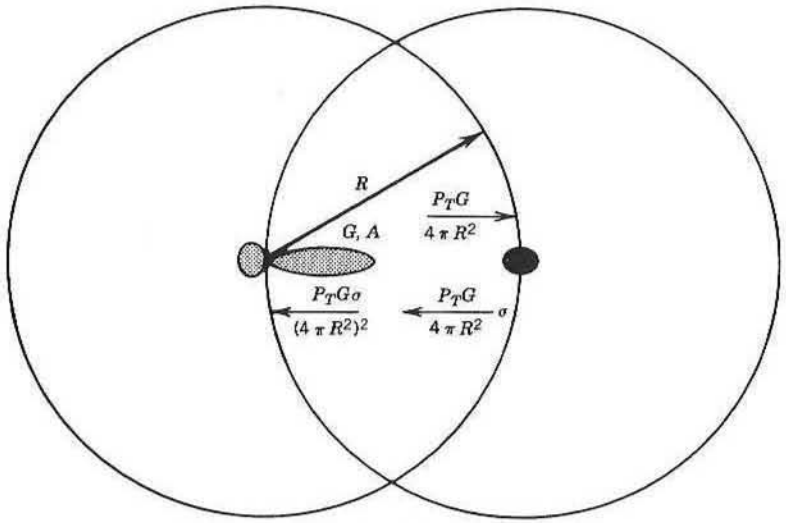

Figure 1.2 *Power densities in the radar scene.*

If the antenna has a gain G, and it is pointing in the direction of the target, then the power density at the target area would be multiplied by G. Now assume that the target reflects back all the power intercepted by its effective area, and the reflection pattern is isotropic. If the effective area of that isotropic target is σ, then the power that it reflects isotropically is given by

$$\text{Reflected power} = \frac{P_T G\sigma}{4\pi R^2}$$

Since the power is reflected isotropically, the reflected power density back at the radar is

$$\text{Reflected power density} = \frac{P_T G\sigma}{(4\pi R^2)^2}$$

If the radar's receiving antenna has an effective area A, then the power received by the antenna is given by

$$P_R = \frac{P_T GA\sigma}{(4\pi R^2)^2} \tag{1.5}$$

In Insert 1B we will show that the relationship between the antenna gain G and its effective area A is given by

$$A = \frac{G\lambda^2}{4\pi} \tag{1.6}$$

Inserting (1.6) in (1.5) yields the basic radar equation

$$P_R = \frac{P_T G^2 \lambda^2 \sigma}{(4\pi)^3 R^4} \tag{1.7}$$

The radar equation was developed assuming a target with area σ and with the rare quality of an isotropic reflection pattern. Most targets are not isotropic. So that we may still be able to use the radar equation, we will replace each real target with an isotropic target and change the area of the isotropic target until it produces the same return power as the original target. Thus, σ is the area of a target that reflects back isotropically and would have caused the same return power as the original target.

The σ area of a target is called its *radar cross section*. Usually the physical area of a real target will be quite different from its σ. Furthermore, most targets exhibit different σ's at different aspect angles and at different frequencies. The next chapter is devoted to the issue of radar cross section. Table 1.1 lists typical values of σ for several targets.

Table 1.1 Typical Values of Radar Cross Section

Target	σ (m^2)
Insect	10^{-5}
Bird	0.01
Small missile	0.1
Man	1
Small aircraft	2
Large fighter	10
Large airliner	40
Car	100

INSERT 1B Antenna Aperture and Gain

A nonrigorous result of the relation between gain and effective aperture will be reached using two parabolic antennas facing each other. In the parabolic reflector shown in Fig. 1.3 it is known that if the feeding is done at the focal point then the wave front is parallel to the vertical line PP'. Toward the tilted direction θ, the additional distance of the path from P' is

$$P'P'' = D \sin\theta \approx D\theta \tag{1B.1}$$

where D is the diameter of the antenna aperture and θ is small.

When that additional distance is equal to $\frac{\lambda}{2}$, the radiation from the two edges of the parabola are out of phase and cancel each other, which hints that the overall radiation in the direction

$$\theta_1 = \frac{\lambda}{2D} \tag{1B.2}$$

is considerably weaker than at $\theta = 0$. We will assume that the radiated power is evenly distributed within the cone defined by $|\theta| < \theta_1$ and is zero outside that cone. Thus, at a distance R from a transmitting parabolic antenna with diameter D_T, the power is evenly distributed over a circular area whose diameter is $R\lambda/D_T$ (Fig. 1.4). If a receiving parabola with diameter D_R is placed at distance R, then the received power will be

$$\frac{P_R}{P_T} \approx \frac{D_R^2}{(R\lambda/D_T)^2} \tag{1B.3}$$

Converting from diameter to area we can rewrite (1B.3) as

$$\frac{P_R}{P_T} \approx \frac{16A_RA_T}{\pi^2(R\lambda)^2} = 1.62\frac{A_RA_T}{(R\lambda)^2} \tag{1B.4}$$

The factor 1.62 is the result of our various simplifying assumptions. The exact factor is 1. Hence

$$\frac{P_R}{P_T} = \frac{A_RA_T}{(R\lambda)^2} \tag{1B.5}$$

On the other hand, we showed that the received (and reflected) power by an area $A_R = \sigma$ is given by

$$\frac{P_R}{P_T} = \frac{A_RG_T}{4\pi R^2} \tag{1B.6}$$

Equating (1B.5) to (1B.6) and dropping the subscript T, we obtain

$$A = \frac{G\lambda^2}{4\pi} \tag{1B.7}$$

A dipole can provide a check for (1B.7). In a dipole it is well known that $G = 1.5$ and $A = 0.119\lambda^2$. Indeed, $1.5/(4\pi) = 0.119$.

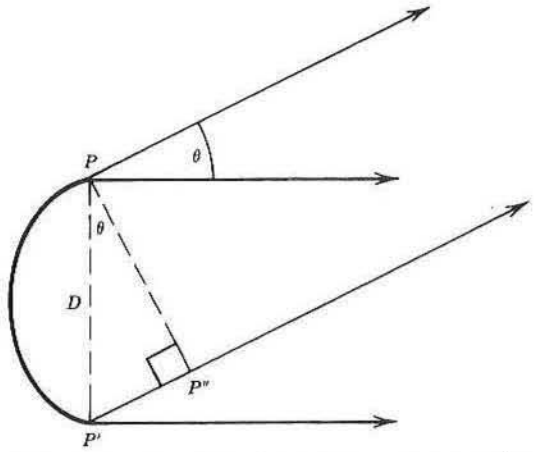

Figure 1.3 Path differences from the antenna aperture edges to a tilted direction.

Another form of the radar equation is the SNR as function of range. In order to develop this form it will be helpful first to define a signal. Later it will be shown that the equation is universal for all signals. Let the signal be a train of coherent RF pulses, at the carrier frequency f_C, as shown in Fig. 1.5.

A nearly optimal receiver for the detection of the pulse train is shown in Fig. 1.6. It comprises a narrow-band filter "matched" to the single-pulse

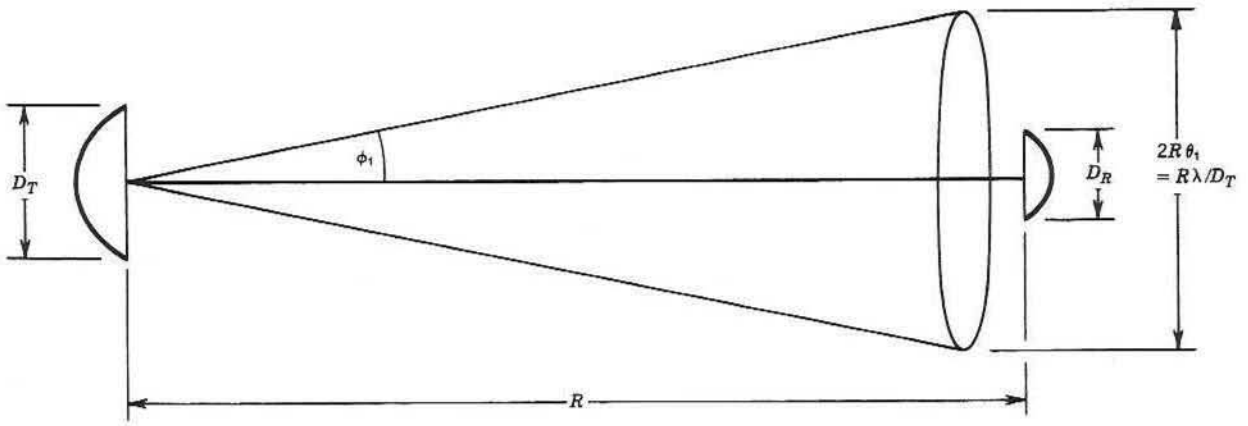

Figure 1.4 *Illumination geometry between two parabolic antennas.*

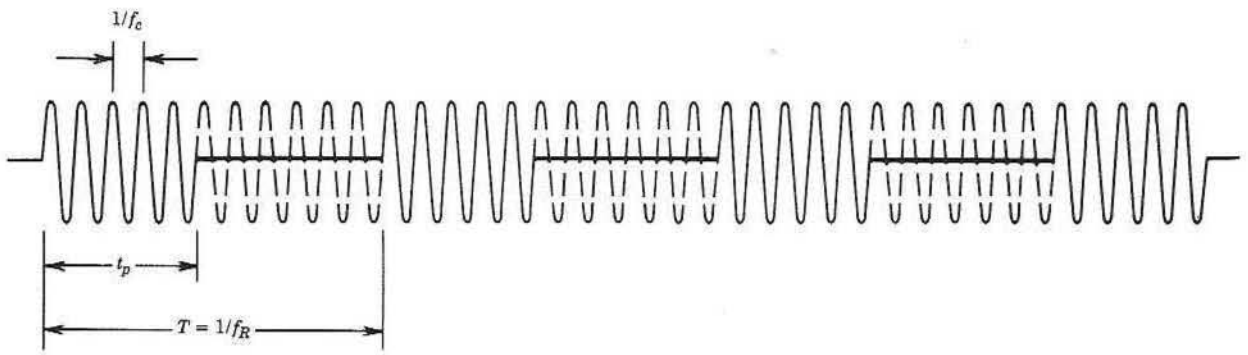

Figure 1.5 *A coherent pulse train.*

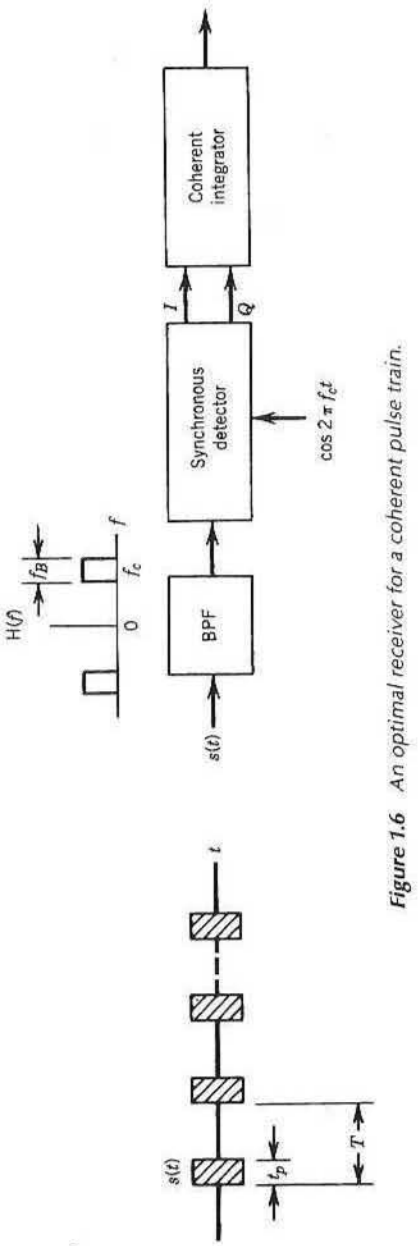

Figure 1.6 An optimal receiver for a coherent pulse train.

width, followed by a synchronous detector and an integrator. The topic of matched filters will be discussed separately in a later chapter. Here it will suffice to mention that a bandpass filter with a rectangular response over the bandwidth f_B (in hertz) is a good representative of a matched filter to a single pulse of duration t_p, if the bandwidth is related to the pulse duration as

$$f_B = \frac{1}{t_p} \tag{1.8}$$

The thermal noise power after such a filter is given by

$$N = FKT_E f_B = N_0 f_B \tag{1.9}$$

where

F is the receiver noise figure,
K is Boltzmann's constant ($= 1.38 \times 10^{-23}$ W · s/°K),
T_E is the temperature in degrees Kelvin,
N_0 is the noise (one-sided) spectral power density in watts per hertz.

Having the noise power (1.9) and the signal power (1.7), it is now possible to write the radar equation in terms of signal-to-noise ratio

$$\text{SNR}_P = \frac{P_T G^2 \lambda^2 \sigma}{(4\pi)^3 R^4 N_0 f_B} \tag{1.10}$$

SNR_P is the signal-to-noise power ratio when only one pulse is returned from the target. Normally the target is illuminated for a relatively long period of time T_I, and the number of pulses that can be used is M, where

$$M = T_I f_R \tag{1.11}$$

and where f_R is the pulse repetition frequency.

The synchronous detector used in the receiver maintains phase information [through the in-phase (I) and the quadrature (Q) components] and therefore allows coherent integration of the M pulses. The issue of coherent and noncoherent integration will be further discussed in the chapter on radar detection. Here it will suffice to mention that the SNR of M coherently integrated pulses is M times the SNR of a single pulse; that is,

$$\text{SNR} = M\,\text{SNR}_P \tag{1.12}$$

Noting that the average transmitted power is given by

$$P_{\text{AVE}} = P_T t_P f_R = P_T \frac{M}{f_B T_I} \tag{1.13}$$

and using it and (1.10) in (1.12) yields

$$\text{SNR} = \frac{P_{\text{AVE}} T_I G^2 \lambda^2 \sigma}{(4\pi)^3 R^4 N_0} \tag{1.14}$$

Note that $P_{\text{AVE}} T_I$ is the energy transmitted by the radar during the illumination time of the target, and it is this energy that determines the SNR that results from optimal processing of the signal during the entire target illumination time.

To show that (1.14) is independent of the type of signal, let us transmit a CW signal for the entire illumination time. This signal can be treated as one pulse of duration T_I. We can therefore use (1.10) with the following replacements:

$$\text{SNR}_P = \text{SNR}, \quad P_T = P_{\text{AVE}}, \quad f_B = \frac{1}{T_I} \tag{1.15}$$

which will also yield (1.14).

The illumination time of a point target by a scanning radar is a function of the antenna scan rate and the antenna beamwidth in the scan plane. The antenna beamwidth is obviously related to the antenna gain. A simple relationship can be deduced from realizing that there are $4\pi(180/\pi)^2 = 41{,}253$ square degrees in a sphere. An antenna with 3-dB beamwidths θ_H and θ_V, in the two principal planes, radiates into $\theta_H \theta_V$ square degrees out of a total of 41,253. The antenna efficiency ρ_A is usually about 0.5. Thus

$$G \approx \frac{41{,}253}{\theta_H \theta_V} \rho_A \approx \frac{20{,}000}{\theta_H \theta_V} \tag{1.16}$$

where θ_H and θ_V are in degrees. When θ_H and θ_V are in radians,

$$G \approx \frac{4\pi}{\theta_H \theta_V} \rho_A \tag{1.17}$$

Another form of the radar equation is suitable for a surveillance radar, which scans a two-dimensional angular region of Ω square radians. If the total scan time is t_S, then the target illumination time is given by,

$$t_I \approx t_S \frac{\theta_H \theta_V}{\Omega} \approx t_S \frac{4\pi\rho_A}{\Omega G} \tag{1.18}$$

Using (1.18) and (1B.7) in (1.14) yields

$$\text{SNR} = \frac{P_{\text{AVE}} A \sigma \rho_A}{4\pi R^4 N_0} \frac{t_S}{\Omega} \tag{1.19}$$

Equations (1.12), (1.14), and (1.19) assumed coherent integration of the received signal over the entire illumination time. If this is not the case, then the radar equation should be modified to include an integration loss. The integration loss will be discussed in more detail in the chapter on radar detection. Integration loss and antenna efficiency are not the only losses that should be accounted for in the radar equation. For example, a loss term should be added because of the erroneous assumption that the radiation pattern is uniform over the antenna beamwidth. A very practical loss is due to attenuation and mismatch in the transmission line. A practical discussion of most loss factors can be found in [1]. It is customary to include all the losses in one coefficient L (> 1), which appears in the denominator of the radar equation. Since L covers also the antenna efficiency, Eq. (1.19) will be rewritten as

$$\text{SNR} = \frac{P_{\text{AVE}} A \sigma}{4\pi R^4 N_0 L} \frac{t_S}{\Omega} \tag{1.20}$$

The loss term L should appear also in the other versions of the radar equation—in particular, Eq. (1.14).

We will conclude the first chapter with a discussion of radar propagation velocity and direction as they behave in a real atmosphere.

ELECTROMAGNETIC PROPAGATION IN THE REAL ATMOSPHERE

The propagation velocity in any homogeneous medium is given by

$$C_P = \frac{C}{n} \tag{1.21}$$

where n is the refractive index. Since n is very close to one, it is more convenient to use N, defined by

$$N = (n - 1)10^6 \tag{1.22}$$

A common semiempirical expression for N is

$$N = \frac{77.6}{T}\left(P + 4810\frac{e}{T}\right) \tag{1.23}$$

where

T is the air temperature in degrees Kelvin,
P is the air pressure in millibars,
e is the water vapor pressure in millibars.

Table 1.2 Refraction Index as a Function of Height for a Standard Atmosphere

h (km)	N	$N_S - [h/(4a)]10^6$
0	$319 = N_S$	319
1	277	279
3	216	201
10	92	—
20	20	—
50	0.2	—

All three parameters affecting N are usually changing with altitude. At a given altitude, they also change with the weather conditions. Assuming standard atmosphere, the average N as function of the altitude h, is given in Table 1.2.

The last column is an empirical fit for the measured change of N with altitude (a is the earth radius $\approx$ 6370 km). The fit is good to an altitude of about 5 km. This linear model of the refractive index with height is also called the effective 4/3 earth radius model and will be described later in this chapter.

Since N changes with altitude, ray propagation will suffer bending unless its direction is perpendicular to the earth surface. Thus, the antenna's pointing direction, based on maximum signal, will not necessarily indicate the correct geometrical direction to the target. Maximum bending occurs when the radar looks toward the horizon. It is well known that the apparent sun at sunset is seen between 0.5° and 1° above its true direction. Tables for the elevation angle error [2], for a target at a height of 70 km (practically outside the atmosphere), indicate an elevation error of 0.92° for an initial elevation of 0°, and an error of 0.24° for an initial elevation of 3°. Exact calculations of the bending and the elevation angle error involve complicated ray tracing. The linear model, however, yields relatively simple expressions, which are summarized below, with the geometry as defined in Fig. 1.7.

In Fig. 1.7 the radar is on the surface of the earth at point S, where the index of refraction is n_S. The target is at point T, at an altitude h above the spherical earth. The index of refraction n is spehrically stratified and concentric with the earth. The trace of the ray from S to T (heavy line) is bent. The initial elevation angle is θ_0. The local elevation angle at T is θ. The bending α is the angle between the tangents to the ray at S and at T. The elevation angle error ε is the angle between the tangent to the ray at S and the straight line connecting S to T.

We will begin our analysis with two results of geometrical optics. From Snell's law for polar coordinates we have

$$n_S a \cos\theta_0 = n(a + h)\cos\theta \tag{1.24}$$

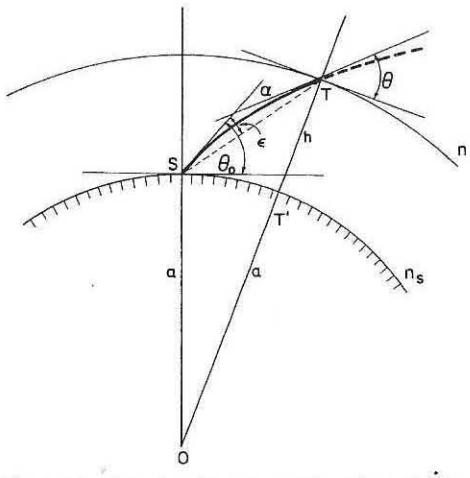

Figure 1.7 *The geometry of radio propagation through the atmosphere.*

From Snell's law and the geometry it can be shown [2] that

$$\frac{d\alpha}{dn} = -\frac{\cot\theta}{n} \tag{1.25}$$

and since n is very close to one,

$$\frac{d\alpha}{dn} \approx -\cot\theta \tag{1.26}$$

The simplified analysis is based on the linear model of the refractive index as function of height

$$n = n_S - \frac{h}{4a} \tag{1.27}$$

which yields

$$\frac{dn}{dh} = -\frac{1}{4a} \tag{1.28}$$

Using the linear model in (1.24), and bearing in mind that $n_S \approx 1$, $h \ll 1$, we get

$$\frac{\cos\theta}{\cos\theta_0} \approx \frac{\frac{4}{3}a}{\frac{4}{3}a + h} \tag{1.29}$$

Equation (1.29) is what gave the linear model its other name—the effective 4/3 earth radius model. Note that Snell's law (1.24) for an earth with an atmosphere that has a constant index of refraction ($n = n_S$), and a radius $4a/3$, would reduce to (1.29). Over such an earth, there will be no ray bending.

For small θ, Eq. (1.29) becomes

$$\theta^2 \approx \theta_0^2 + \frac{3h}{2a}, \qquad \theta \ll 1 \text{ rad} \tag{1.30}$$

Also for small θ, Eq. (1.26) becomes

$$\frac{d\alpha}{dn} \approx -\frac{1}{\theta}, \qquad \theta \ll 1 \text{ rad} \tag{1.31}$$

Using (1.28) and (1.30) in (1.31) and integrating, we obtain

$$\alpha \approx \int_0^h \frac{dh}{4a\left(\theta_0^2 + 3h/2a\right)^{1/2}} \tag{1.32}$$

For the special case in which $\theta_0 = 0$, Eq. (1.32) can be solved explicitly, yielding

$$\alpha \approx \left(\frac{h}{6a}\right)^{1/2}, \qquad \theta_0 = 0 \tag{1.33}$$

In (1.33) we have obtained an approximate simple expression for the bending of a beam pointed toward the horizon. It should be emphasized again that many simplifying assumptions were made in order to obtain the simple expression of (1.33), beginning with the linear model of the refraction index and ending with a horizontal pointing ray.

A plot of (1.33) (bending as function of height) is given in Fig. 1.8, next to the direct integration of (1.25) using (1.24) and the linear model given in (1.27). The two curves are indeed very close to each other.

The linear model predicts $n < 1$ above $h = 8$ km, which, of course, cannot be correct. A model that avoids this problem is the exponential model given by

$$N = N_S \exp(-0.1439h) \tag{1.34}$$

where h is the altitude (in kilometers). A plot of the expected bending as function of the target's height, for the exponential model, is also given in Fig. 1.8. Note that both the linear model and the exponential model, used in Fig. 1.8, assumed $N_S = 319$. Note also that Fig. 1.8 is for a horizontal pointing beam—namely, $\theta_0 = 0$.

The elevation angle error ε is different from the bending angle α. An exact expression for the elevation angle error as function of θ, α, n_S, and n is given in the problems of this chapter. Here we will only point out that

$$\alpha/2 \le \varepsilon \le \alpha \tag{1.35}$$

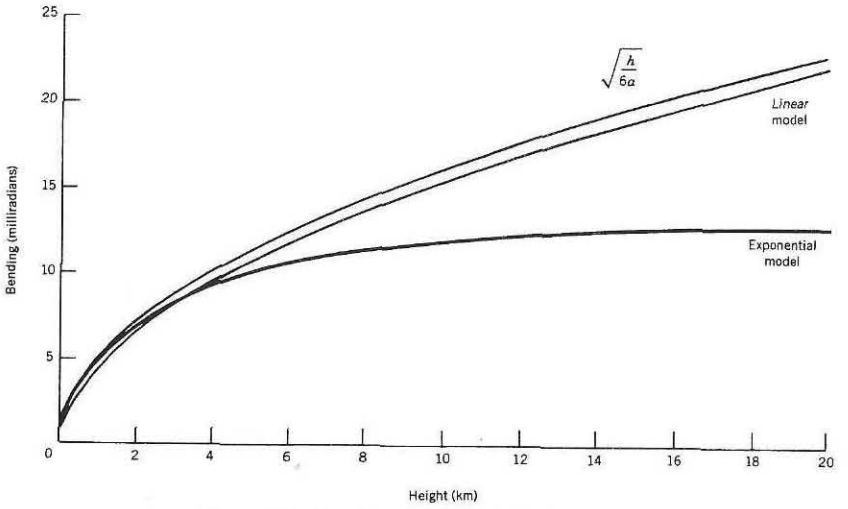

Figure 1.8 *Ray bending vs. height for* $\theta_0 = 0$.

Our limited discussion of electromagnetic propagation in the real atmosphere ends here. There are many other topics such as more accurate refractive index models, ducting effects, and attenuation by atmospheric gases and by rain. The interested reader is referred to [2] and [3].

REFERENCES

1.1 Merril I. Skolnik, *Introduction to Radar Systems*, 2nd ed., McGraw-Hill, New York, 1980.

1.2 B. R. Bean and E. J. Dutton, *Radio Meterology*, Dover, New York, 1968.

1.3 Lamont V. Blake, *Radar Range-Performance Analysis*, Heath, Lexington, Massachusetts, 1980.

PROBLEMS

1.1 What will be the Doppler frequency when there is target acceleration (namely, $\ddot{R} \neq 0$)?

1.2 For the Doppler shift from a moving target if relativistic effects are considered, the received frequency is given by

$$f_R = f_T \frac{1 - \dot{R}/C}{1 + \dot{R}/C}$$

For an electromagnetic wave and target radial velocity of 300 m/s, compare this expression to the simplified one (1.3).

1.3 If police radars were using acoustic signals (whose velocity of propagation is 333 m/s), and a car was traveling away from the radar at a speed of 120 km/h, what would be the measurement error if the relativistic effect (see Problem 1.2) was ignored?

1.4 A radar with antenna gain G_1 is illuminating a target antenna whose gain (pointing toward the radar) is G_2. A receiver is connected at the target antenna. Half the power received by the target antenna is forwarded to the receiver and the other half is reflected back to the radar.

(a) Find an expression for the ratio between the power received by the target receiver and the power received by the radar.

(b) What is the ratio, in decibels, when $G_1 = G_2 = 100$ and $R/\lambda = 10^4$?

1.5 Police radar is designed to receive a return from a car, with a radar cross section σ, up to a distance of $R_M = 50$ m. The car is equipped with a radar detector. The effective area of the detector antenna is $k\sigma$ ($k = 0.001$). The other radar parameters are $G = 100$ and $\lambda = 0.02$ m. Assuming that the car's radar detector has the same sensitivity as the radar receiver, at what distance will the radar detector provide a warning?

1.6 The radar parameters are: $P_{AVE} = 1$ kW, $T_I = 0.05$ s, $F = 5$, $\lambda = 0.2$ m, and $G = 100$. What is the range from which a target with $\sigma = 10$ m^2 will yield an SNR of 20 dB?

1.7 Find the ground distance to the radar horizon from an antenna at height h. Assume the linear model of the refractive index.

1.8 N_S of 319 was obtained for the standard surface parameters: $T = 288°$K, $P = 1013$ mb, and $e = 10.2$ mb. Find the (separate) effects of the following practical meteorological changes on N_S: $\Delta T = 10°$, $\Delta P = 10$ mb, and $\Delta e = 3$ mb.

1.9 Prove that the elevation angle error is given by

$$\tan \varepsilon = \frac{\cos \alpha - \sin \alpha \tan \theta - (n/n_S)}{(n/n_S)\tan \theta_0 - \sin \alpha - \cos \alpha \tan \theta}$$

1.10 Extend Table 1.2 by adding a column for the exponential model.

2 Cross Section of Radar Targets

A major parameter in the radar equation is the target's radar cross section (σ). A verbal definition of σ was given in Chapter 1. There is some correlation between σ and the size of the target, but other factors such as configuration, aspect angle, and wavelength also affect its value. In this chapter we will discuss deterministic expressions of σ for some simple geometrical bodies and several common statistical behaviors of more complex targets.

SPHERES

The cross section σ of a sphere of radius a is shown in Fig. 2.1 as function of the circumference (normalized with respect to λ). In the optical region (large spheres) the asymptotic expression is given by

$$\sigma = \pi a^2, \qquad \lambda \ll a \tag{2.1}$$

For small spheres (Rayleigh region) the asymptotic expression is

$$\sigma = \pi a^2 9(ka)^4, \qquad a \ll \lambda \tag{2.2}$$

where

$$k = \frac{2\pi}{\lambda} \tag{2.3}$$

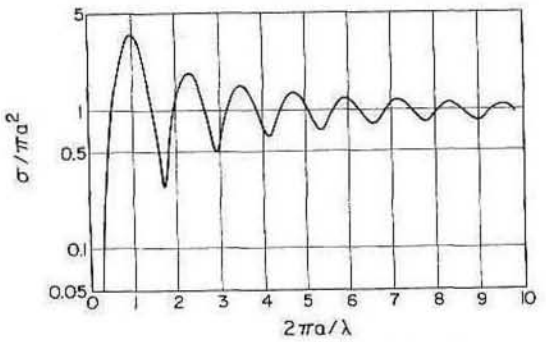

Figure 2.1 *Radar cross section of a sphere.*

In between these two regions lies the resonance (Mie) region, in which the behavior is indeed oscillatory, with a peak of approximately 3.6 at $a = \lambda/2\pi$. The resonant mode is explained by a creeping wave that travels around the rear of the sphere and adds constructively or destructively to the specular reflection from the front of the sphere. Whether the addition is constructive or destructive depends on the additional distance traveled by the creeping wave, which is a function of the radius of the sphere.

It should be noted that because of its symmetrical shape, a sphere exhibits the same σ at all aspect angles, and that σ is very well known. Furthermore, in the optical region σ is independent of λ. Thus a sphere can serve as a good calibration device in radar measurements.

The general approximations for the Rayleigh and optical regions are as follows:

In the *Rayleigh* region of a rounded smooth object of volume V

$$\sigma \approx \frac{4k^4V^2}{\pi} \tag{2.4}$$

In the *optical* region of a smooth curved surface normal to the incident wave, in which a_1 and a_2 are the two radii of curvature of the surface,

$$\sigma \approx \pi a_1 a_2 \tag{2.5}$$

Setting $a_1 = a_2 = a$ in (2.5) will yield (2.1); however, (2.4) differs from (2.2) in the coefficient, which is 64/9 rather than 9.

PLANAR SURFACES

When a large, smooth surface is placed perpendicular to the range vector from the radar (i.e., normal incidence), and its area is A, then its effective aperture, which intercepts the power flux density, is also A. If that power is reflected

isotropically then σ will be equal to A. But a large smooth surface reflects most of the power back in the perpendicular direction, with a gain related to the aperture A, as was calculated in Insert 1A as follows:

$$G = \frac{4\pi A}{\lambda^2} \tag{2.6}$$

Thus, the effective cross section of a large, smooth plane in the normal direction is

$$\sigma = AG = \frac{4\pi A^2}{\lambda^2}, \qquad 2\pi A^{1/2} \gg \lambda \tag{2.7}$$

The question of what is "smooth" will be discussed in Chapter 4. Equation (2.7) says that σ of a large plane is much larger than the area A of that plane, but only at a normal incidence.

At other than normal incidence the dependence of σ on the angle of incidence Θ (measured from the normal), for a *square* flat plate is given by [1] as

$$\sigma = \frac{4\pi a^4}{\lambda^2}\left[\frac{\sin(ka\sin\Theta)}{ka\sin\Theta}\right]^2 \tag{2.8}$$

where a is the length of the side. For a *circular* flat plate,

$$\sigma = \frac{\pi a^2}{\tan^2\Theta}\left[J_1(2ka\sin\Theta)\right]^2 \tag{2.9}$$

where a is the radius of the disk and $J_1(x)$ is the Bessel function of the first order.

Note that (2.8) reduces to (2.7) at $\Theta = 0$, but drops off rapidly, following the $(\sin x)/x$ shape, with a first null at $\Theta = \lambda/(2a)$ radians. For $a = 10\lambda$, the first null occurs at $\Theta = 2.9°$. Thus we see that the large backscattering of a flat plate has a pattern that becomes narrower the larger the plate is. When it is desired to take advantage of this large σ at other than normal incidence, it is possible to use a corner reflector.

CORNER REFLECTORS

A corner reflector can provide a large cross section over a wide range of aspect angles. A cut along a dihedral corner is shown in Fig. 2.2, in which the reflection concept is also demonstrated. The ray tracing shows that whatever the incident angle, after two specular reflections the reflected ray is always parallel to the incident ray. However, the area that participates in the

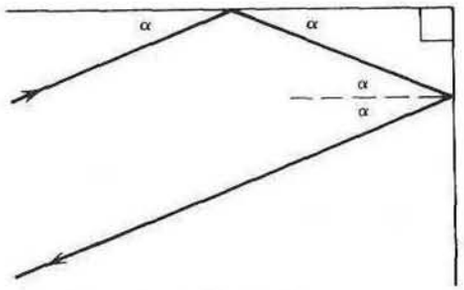

Figure 2.2 *Reflection from a corner.*

reflection process and its projection on the plane normal to the incidence are maximum at $\alpha = 45°$ and drops in either direction. This area is called the effective area. If the dihedral corner is symmetrical with width a (of each wall) and height b, then the effective area is given by

$$A_{\text{EFF}} = 2ab \sin \alpha, \qquad 0 \le \alpha \le 45° \tag{2.10}$$

The cross section is related to the effective area approximately as if it were the area of a perpendicular large plane [see (2.7)]; hence

$$\sigma \approx \frac{4\pi A_{\text{EFF}}^2}{\lambda^2} \tag{2.11}$$

Using (2.10) in (2.11) will yield an approximate expression for the cross section of a dihedral corner reflector; that is,

$$\sigma \approx \frac{16\pi a^2 b^2}{\lambda^2} \sin^2 \alpha, \qquad 0 \le \alpha \le 45° \tag{2.12}$$

For $45° \le \alpha \le 90°$ use $90° - \alpha$ instead of α.

Setting $\alpha = 45°$ in (2.11) will yield the maximum cross section available from a dihedral corner reflector (see Fig. 2.3a):

$$\sigma_{\text{MAX}} \approx \frac{8\pi a^2 b^2}{\lambda^2} \quad \text{(dihedral)} \tag{2.13}$$

Equation (2.12) ignores the fact that at $\alpha = 0$ there is normal incidence on one of the walls of the corner reflector, which should yield the strong, flat plate reflection rather than the zero reflection predicted by (2.12). Furthermore, this flat plate reflection should extend to small negative α, until the shadowing effect of the other wall becomes significant. Note also that the flat plate reflection blends with the dihedral reflection without a phase (delay) step. A model suggested in [2] for a square dihedral is

$$\sigma = \left(\sqrt{\sigma_D} + \sqrt{\sigma_{\text{PF}}}\right)^2 \tag{2.14}$$

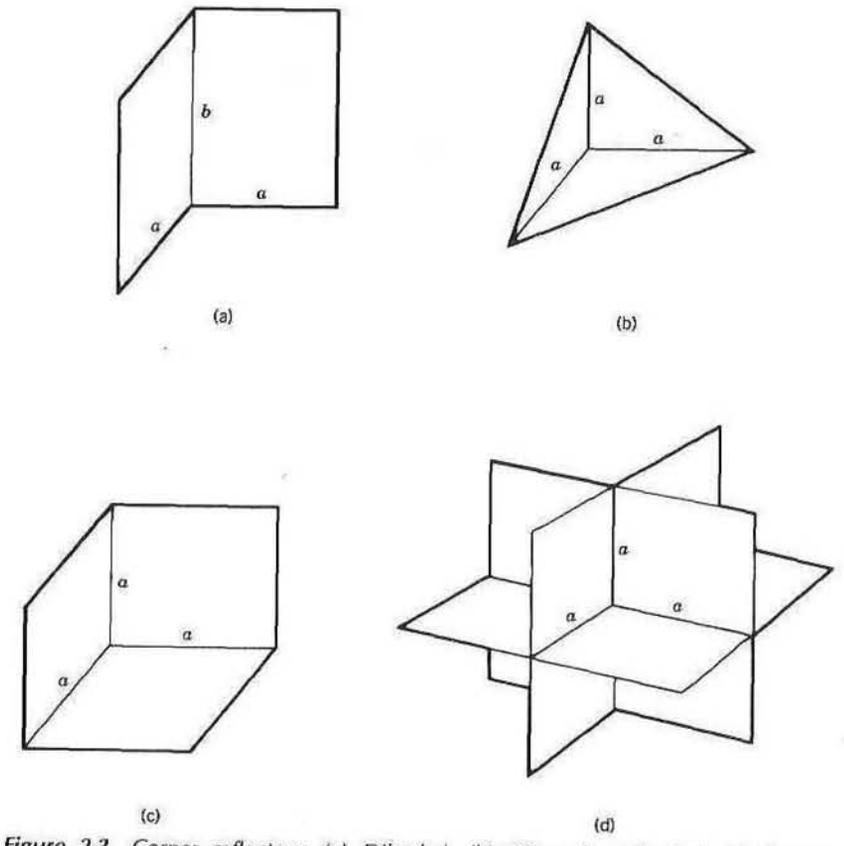

Figure 2.3 *Corner reflectors: (a) Dihedral. (b) Triangular trihedral. (c) Square trihedral. (d) Retroflector.*

where

$$\sigma_D = \frac{16\pi a^4}{\lambda^2} \sin^2 \alpha, \qquad 0 \le \alpha \le 45°, \quad \text{zero elsewhere}$$

and

$$\sigma_{\text{PF}} = \frac{4\pi a^4}{\lambda^2} \left(\frac{\sin(ka \sin \alpha)}{ka \sin \alpha} \right)^2, \qquad -20° \le \alpha \le 45°, \quad \text{zero elsewhere}$$

A plot of (2.14) is given in Fig. 2.4 for a case in which $a = 15\lambda$. Despite its simplicity, the model agrees fairly well with measurements.

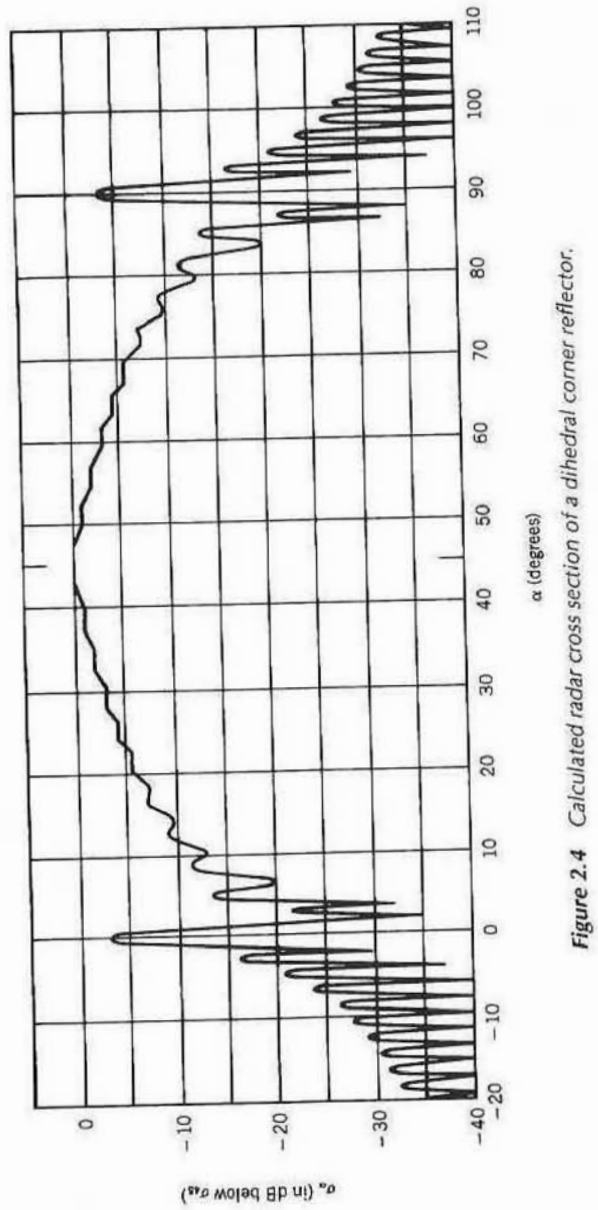

Figure 2.4 Calculated radar cross section of a dihedral corner reflector.

The reflection from a dihedral corner reflector is insensitive to the incidence angle in only one plane (e.g., azimuth). To extend this quality to the other plane (e.g., elevation) it is necessary to use a trihedral reflector. There are several configurations of trihedral corner reflectors. Two are shown in Fig. 2.3. The triangular trihedral (Fig. 2.3b) has a maximum radar cross section of

$$\sigma_{MAX} \approx \frac{4\pi a^4}{3\lambda^2} \quad \text{(triangular trihedral)} \tag{2.15}$$

and its angular coverage can be described by a 3-dB drop at about 20° off the symmetry axis. The square trihedral (Fig. 2.3c) has a larger maximum cross section (but narrower angular coverage); that is,

$$\sigma_{MAX} \approx \frac{12\pi a^4}{\lambda^2} \quad \text{(square trihedral)} \tag{2.16}$$

where a is defined in Fig. 2.3.

In order to yield complete spherical coverage, at least eight trihedrals are necessary (Fig. 2.3d). Such a body is called a retroflector. Retroflectors are used extensively to enhance friendly radar returns.

RADAR CROSS SECTION OF ANTENNAS

Many drivers have noticed the strong reflection from the eyes of a cat caught in the light beam of their car at night. The same phenomenon makes antennas strong backscatterers when they face the radar. The backscattering from antennas is also strongly dependent on the load at the antenna terminals. This can be explained by the part of the power received by the antenna and either absorbed in the load, if it is well matched to the antenna impedance, or reflected back and retransmitted, with some phase and amplitude changes. The retransmitted field may be constructively or destructively added to the portion of the field directly reflected from the antenna structure. The ability to affect the backscattering of antennas by changing their load can be used in several ways. One use is to mark a specific return relative to other undesired (clutter) returns by modulating the scatterer using impedance switching. Such modulated scatterers are used in microwave measurements [3]. Modulated scatterers are also used for calibration and testing of Doppler radars, by setting the modulation rate at the expected Doppler rate. A completely opposite application is to impedance-load an antennalike reflector to reduce its radar cross section.

Here we will deal only with the most basic antenna—the dipole. Dipole backscattering and the effect of different loading at its center were studied by Harrington [4] and Harrington and Mautz [5]. They showed that the radar

cross section of a *short-circuited* small dipole of length L and wire radius a is given by

$$\sigma \approx \frac{0.176\lambda^2}{1 + 12^2(kL)^{-6}[3\ln(2L/a) - 7]^2}, \qquad \frac{L}{\lambda} < 0.4 \tag{2.17}$$

For a small *open-circuited* dipole, σ is given by

$$\sigma \approx \frac{\lambda^2(kL)^6}{96^2\pi[\ln(L/a) - 2]^2}, \qquad \frac{L}{\lambda} < 0.8 \tag{2.18}$$

Both dipoles can reach resonance. At resonance the cross section is given by

$$\sigma = 0.716\lambda^2 \tag{2.19}$$

The shorted dipole reaches resonance when $L \approx 0.45\lambda$, and the open-circuited dipole reaches resonance when $L \approx 0.87\lambda$. Small dipoles of other lengths can be resonated by loading them with the appropriate inductive reactance. At resonance they will also exhibit the maximum σ given by (2.19).

Comparing (2.19) to (2.18) we note that a thin dipole ($L/a = 150$) of length $L = 0.45\lambda$, when its load is switched from a short circuit to an open circuit, exhibits a drop in its σ/λ^2 from 0.716 down to 0.002, namely a drop of 26 dB.

Finally, note that the dipole gain is $G = 1.5$, and that $0.716 = 1.5^2/\pi$. Thus (2.19) can be written as

$$\sigma = \frac{\lambda^2 G^2}{\pi} \tag{2.20}$$

This relationship between the antenna gain and its radar cross section is a good approximation for other antennas as well.

MULTIPLE SCATTERERS

When several scatterers contribute to the return, they should be added vectorially, taking into consideration the phase differences. Because σ is related to power, whereas phase is a quality of fields or voltages, the quantity that will be associated with phase and vector sum will be $\sqrt{\sigma}$. In general the total radar cross section of M scatterers is given by

$$\sigma = \left| \sum_{n=1}^{M} \sqrt{\sigma_n} \exp \frac{j4\pi R_n}{\lambda} \right|^2 \tag{2.21}$$

where σ_n and R_n are, respectively, the cross section of and the range to the

nth individual scatterer. Note that the round-trip distance is accounted for in the exponent by having a 4π rather than a 2π factor. The model in (2.21) ignores shadowing and multiple reflections between the individual scatterers.

For a multiple-scatterers target, if the number of scatterers is larger than two and the spacing is longer than few wavelengths, then the total cross section becomes strongly dependent on aspect angle and there is a very complicated scattering pattern. To demonstrate such a pattern we have calculated the total cross section of five scatterers located on a plane, at the Cartesian coordinates $(2,0)$; $(1,3)$; $(-1,1)$; $(-3,-2)$; and $(0,-2)$. The wavelength is 0.28 (in the same units). To simplify the analysis the individual scatterers were chosen to be spheres, which exhibit no dependence of σ_n on the aspect angle. Furthermore, all spheres are of the same size; that is, $\sigma_n = \sigma_1$.

The resulting two-dimensional pattern of $\sigma(\Theta)/\sigma_1$ in dB, is given in Fig. 2.5. It is clearly a very complicated pattern, with peaks as high as M^2 (14 dB for $M = 5$) and very deep nulls (theoretically there can be nulls down to zero). Furthermore, the angular spacing between peaks and nulls is sometimes only a fraction of a degree.

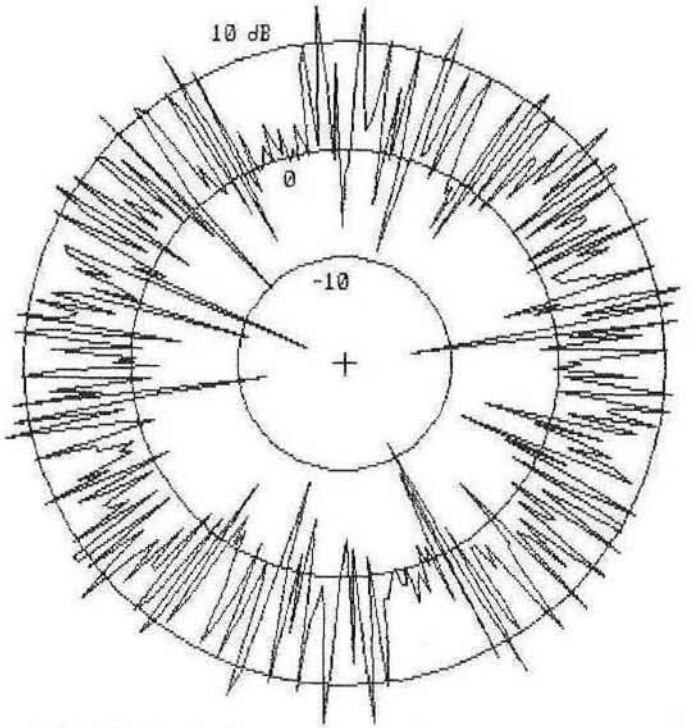

Figure 2.5 *Calculated radar cross section of five point scatterers in a plane.*

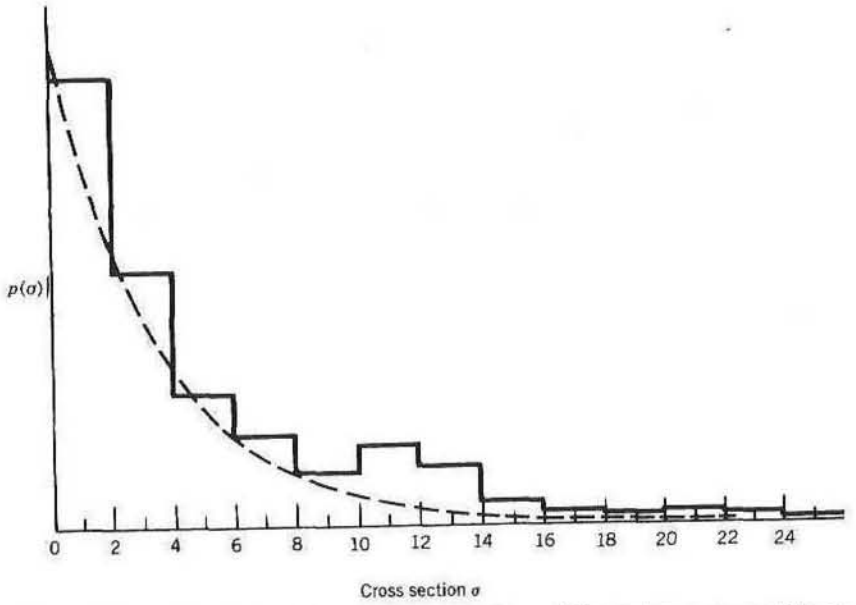

Figure 2.6 *A histogram of the radar cross section of five points compared to an exponential probability density function.*

Considering that this complicated pattern resulted from a rather simple and idealized target (five equal spheres), it is obvious that any real-world multiple-scatterers target (e.g., an aircraft) will yield an even more complicated pattern. For such a target it makes sense to abandon the deterministic approach and to treat its σ as a random variable. Thus we went one step further and calculated the histogram of the 360 values of $\sigma(\Theta)$ obtained at 1° intervals of Θ. ($\sigma_1 = 1$ was chosen.) The result is plotted in Fig. 2.6. Superimposed on it (dotted line) is an exponential probability density function (PDF) given by

$$p(\sigma) = \frac{1}{\bar{\sigma}} \exp \frac{-\sigma}{\bar{\sigma}}, \qquad 0 \le \sigma, \quad \text{zero elsewhere} \tag{2.22}$$

in which $\bar{\sigma} = M\sigma_1 = 5$. Here it suffices to point out the good agreement between the histogram and the exponential PDF. A theoretical justification will be given in the next section.

FLUCTUATING TARGETS

Complex bodies (e.g., aircraft) have been mapped to yield their radar cross section in various planes as a function of the aspect angle. However, because

of their motion relative to the radar, the aspect angle changes, and it may be more practical to describe them in term of the probability density function (PDF) of their σ. The same is true with rough surfaces, such as the ocean or a terrain, which change constantly due to either the surface motion or the radar motion that brings different sections of the surface into view. These kind of targets are called fluctuating targets, and another parameter of importance in their regard is the power-frequency spectrum or the autocorrelation function, which indicates how fast meaningful changes in σ occur.

When the target is constructed from many independently positioned scatterers, the PDF of its σ can usually be described by a *Rayleigh* PDF (for power), also called *exponential* PDF.

$$p_1(\sigma) = \frac{1}{\bar{\sigma}} \exp \frac{-\sigma}{\bar{\sigma}}, \qquad 0 \le \sigma, \quad \text{zero elsewhere} \tag{2.23}$$

where $\bar{\sigma}$ is the average radar cross section. Since σ is linearly related to the received power, (2.23) is the power version of the Rayleigh PDF. To convert to the amplitude version we first note that, ignoring constants, the amplitude A is related to power (and hence to σ) as

$$\sigma = \frac{A^2}{2} \tag{2.24}$$

Hence

$$p_2(A) = \left. \frac{p_1(\sigma)}{|dA/d\sigma|} \right|_{\sigma = A^2/2} \tag{2.25}$$

which yields

$$p_2(A) = \frac{A}{A_0^2} \exp \frac{-A^2}{2A_0^2}, \qquad 0 \le A \tag{2.26}$$

when

$$A_0^2 = \bar{\sigma} \tag{2.27}$$

INSERT 2A Multiple-Scatterers Rayleigh Distribution

In this insert we will present a heuristic analysis that explains the origin of a Rayleigh PDF when the target is constructed from many independently positioned scatterers of similar size. Consider that the radar illuminates an area that can be described by M reflectors. The common illumination means that the antenna beam sees all the M reflectors, and, because of the extended duration of

the transmitted signal, they all contribute to the received signal at a given delay. The difference in the ranges to the various reflectors is expressed in the relative phases of the reflected signals, and the differences in their sizes affect the magnitude of the individually reflected signals. Assume further that because of the roughness of the target area, the range differences to the various reflectors are much larger than the signal wavelength. Because of the modulo 2π nature of the phase term, it is therefore reasonable to assume that the phase of the returns from the various reflectors will be a random variable with a uniform PDF between 0 and 2π.

We can express the signal reflected from the target as a sum of M signals with a common central phase and frequency and with individual amplitudes and additional phases. Thus

$$s_R(t) = \mathrm{Re}\left\{ [\exp(j\omega_c t + j\phi_0)] \sum_{k=1}^{M} a_k \exp(j\phi_k) \right\} \tag{2A.1}$$

The sum in (2A.1) describes the complex envelope of the returned signal and will be termed

$$u = r\exp(j\theta) = \sum_{k=1}^{M} a_k \exp(j\phi_k) \tag{2A.2}$$

Equation (2A.2) can be written as

$$u = \sum_{k=1}^{M} a_k \cos(\phi_k) + j \sum_{k=1}^{M} a_k \sin(\phi_k) \tag{2A.3}$$

We will simplify the assumption that all scatterers contribute more or less equally by choosing

$$a_k = a \tag{2A.4}$$

Thus, (2A.3) reduces to

$$\frac{u}{a} = \sum_{k=1}^{M} \cos(\phi_k) + j \sum_{k=1}^{M} \sin(\phi_k) = X + jY \tag{2A.5}$$

Since ϕ_k is distributed evenly between 0 and 2π, both $\cos(\phi_k)$ and $\sin(\phi_k)$ have a zero mean. For large M, the central limit theorem is satisfied, and both X and Y [defined in (2A.5)] become Gaussian distributions with zero mean and a variance that is M times the variance of $\cos(\phi_k)$. Thus

$$\mathrm{Var}\, Y = \mathrm{Var}\, X = M\int_0^{2\pi} (2\pi)^{-1} \cos^2\phi \, d\phi = \frac{M}{2} \tag{2A.6}$$

X and Y are uncorrelated since, from (2A.5),

$$E\{XY\} = 0 = E\{X\}E\{Y\} \tag{2A.7}$$

Being uncorrelated and Gaussian implies that X and Y are also independent. We can now obtain the PDFs of r and θ. We note that

$$\left(\frac{r}{a}\right)^2 = X^2 + Y^2, \qquad \theta = \arctan\frac{Y}{X} \tag{2A.8}$$

where X and Y are independent Gaussian random variables with zero mean and variance $M/2$. The joint PDF of X and Y is given by

$$p(X,Y) = p(X)p(Y) = \frac{1}{\pi M}\exp\frac{-(X^2+Y^2)}{M} \tag{2A.9}$$

yielding (see, e.g., pp. 145–146 and 96 in [6])

$$p(r) = \frac{2r}{Ma^2}\exp\frac{-r^2}{Ma^2}, \qquad 0 \le r \tag{2A.10}$$

and

$$p(\theta) = \frac{1}{2\pi}, \qquad 0 < \theta < 2\pi \tag{2A.11}$$

Using the transformations

$$A = r\sqrt{2}, \qquad A_0^2 = Ma^2 \tag{2A.12}$$

in (2A.10), we get

$$p(a) = \frac{A}{A_0^2}\exp\frac{-A^2}{2A_0^2}, \qquad 0 \le A \tag{2A.13}$$

which is the Rayleigh PDF (for amplitude) appearing in (2.26).

Our analysis assumed equal contributions from all the scatterers (2A.4), but it can be shown [7] that if the a_k's are samples from a random variable with any PDF, then we still get Rayleigh PDF for the amplitude of the received return.

A plot of $p_2(A)$ is given in Fig. 2.7 (curve II). Note that A_0 is the most probable A. The average, mean-square, and median values of A are, respectively,

$$\overline{A} = A_0(\pi/2)^{1/2} \tag{2.28}$$

$$\overline{A^2} = 2A_0^2 \tag{2.29}$$

and

$$A_M = A_0(\ln 4)^{1/2} \tag{2.30}$$

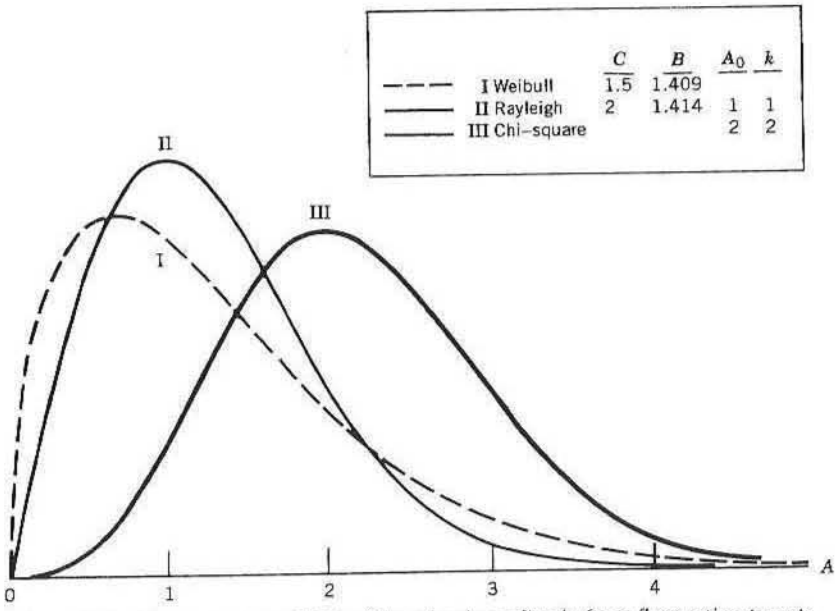

Figure 2.7 *Three common PDFs of the signal amplitude from fluctuating targets.*

The exponential distribution can be seen as a special case from a distribution family called *chi-square*, and described by PDF

$$p_3(\sigma) = \frac{k}{(k-1)!\,\bar{\sigma}}\left(\frac{k\sigma}{\bar{\sigma}}\right)^{k-1} \exp\frac{-k\sigma}{\bar{\sigma}}, \qquad 0 \le \sigma \tag{2.31}$$

Equation (2.26) reduces to (2.23) by choosing $k = 1$. (Recall that $0! = 1$.)

When the reflected signal contains a dominant constant component in addition to a Rayleigh-distributed random component, it can be described by choosing $k = 2$ in the chi-square PDF, which yields

$$p_4(\sigma) = \frac{4\sigma}{\bar{\sigma}^2}\exp\frac{2\sigma}{\bar{\sigma}}, \qquad 0 \le \sigma \tag{2.32}$$

The PDF of the signal amplitude corresponding to $p_4(\sigma)$ is

$$p_5(A) = \frac{9A^3}{2A_0^4}\exp\frac{-3A^2}{2A_0^2}, \qquad 0 \le A \tag{2.33}$$

where A is related to σ as in (2.24). $P_5(A)$ is plotted in Fig. 2.7 as curve III, with a most probable value $A_0 = 2$. Note that the mean value of A is $A_0(3\pi/8)^{1/2}$, and the mean-square value of A is $(4/3)A_0^2$.

As was indicated before, the rate of the fluctuations is also of importance. However, instead of getting into the fine details of the autocorrelation function, it is customary to divide the rate of change into two categories: (a) where there are no changes in the amplitude of all the pulses in a train of pulses (usually the pulses received in one scan of the radar antenna over the target), but that amplitude is a single random variable with one of the PDFs mentioned above; (b) where the amplitude of each pulse in the train is a statistically independent random variable with the same PDF. The first case is called "scan-to-scan fluctuating target", whereas the second case is called "pulse-to-pulse fluctuating target".

Table 2.1 Classification of Fluctuating Targets

Case	k in Eq. (2.31)	Fluctuations Rate
Swerling I	$k = 1$ (Rayleigh)	Scan-to-scan
Swerling II	$k = 1$ (Rayleigh)	Pulse-to-pulse
Swerling III	$k = 2$ (Dominant + Rayleigh)	Scan-to-scan
Swerling IV	$k = 2$ (Dominant + Rayleigh)	Pulse-to-pulse

In addition to the amplitude, we can add an "incoherency" restriction on the initial phase of each pulse—namely, that in both cases the initial phase of each pulse is a statistically independent random variable with a *uniform* PDF. (It is unlikely that the initial phase will remain constant, even when the fluctuations rate is slow.)

So far we have defined two PDFs and two rates of fluctuations, which can yield four combinations. These combinations were studied extensively by Swerling and are named after him, as shown in Table 2.1.

Recently there have been other distributions that were found to fit some measured returns better, particularly sea clutter and rain clouds. For example, the Rayleigh PDF given in (2.26) can be considered to be a special case of a more general family called *Weibull* PDF, given by

$$p_6(A) = \frac{C}{B}\left(\frac{A}{B}\right)^{C-1}\exp\left(\frac{-A}{B}\right)^{C} \qquad 0 < A, \quad 0 < B, \quad 0 < C \tag{2.34}$$

in which A is the signal amplitude, B is a scale parameter, and C is called a shape parameter. Setting $C = 2$ and $B^2 = 2A_0^2$ in (2.34) will yield (2.26). However, some sea clutter and cloud return measurements yielded better fits when C was smaller than 2, and typically between 1.2 and 2. It can easily be shown that the most probable amplitude of the Weibull PDF is given by

$$A_0 = B\left(1 - \frac{1}{C}\right)^{1/C} \tag{2.35}$$

The mean value is given by

$$\bar{A} = B\Gamma\left(1 + \frac{1}{C}\right) \tag{2.36}$$

where $\Gamma(\ )$ is the gamma function. The median value is given by

$$A_M = B(\ln 2)^{1/C} \tag{2.37}$$

The mean-square value is given by

$$\overline{A^2} = B^2\Gamma\left(1 + \frac{2}{C}\right) \tag{2.38}$$

and the variance by

$$\text{Var}\, A = B^2\left[\Gamma\left(1 + \frac{2}{C}\right) - \Gamma^2\left(1 + \frac{1}{C}\right)\right] \tag{2.39}$$

Another interesting feature of the Weibull PDF is the fact that the PDF of the power (σ) that yields the Weibull PDF of the amplitude (A) is also Weibull and has the same form but different constants. Thus, replacing A with σ and setting $C = 1$ and $B = \bar{\sigma}$ in (2.34) will yield (2.23), which is the Rayleigh PDF for power.

A plot of $p_6(A)$, according to (2.34), appears as curve I in Fig. 2.7. The shape parameter was chosen as $C = 1.5$, and B was then calculated ($B = 1.4086$) in order to yield the same mean-square value as the Rayleigh PDF (curve II).

A useful feature of the Weibull PDF is the fact that its constants can be determined from the straight line

$$Y = CX - C \ln B \tag{2.40}$$

where

$$X = \ln A \tag{2.41}$$

and

$$Y = \ln\left\{-\ln\left[1 - \int_0^A p_6(A)\, dA\right]\right\} \tag{2.42}$$

Note that the integration is performed on the *measured* PDF.

Results of measurements [8] of sea clutter at low grazing angles, between 0.5° and 0.72°, for sea state 3 reveal an excellent fit to a straight line, which confirms that a Weibull PDF is a good model for the measured sea clutter. The slope of the straight line yields (for this case of sea clutter) a shape factor $C = 1.585$.

Another PDF sometimes used to fit sea clutter data is the *log-normal* PDF

$$p_7(A) = \frac{1}{\beta A(2\pi)^{1/2}} \exp \frac{-(\ln A - \alpha)^2}{2\beta^2} \tag{2.43}$$

The log-normal PDF obtained its name from the fact that if $\ln A$ is considered to be the variable

$$Y = \ln A \tag{2.44}$$

then $p(Y)$ is a normal PDF with a mean α and a standard deviation β. Like Weibull PDF, log-normal PDF has the same form for the PDFs of the amplitude A and the power σ. Clutter sea return of high-resolution radar showed very good fit to the following representation of a log-normal PDF of σ

$$p_7(\sigma) = \frac{1}{\beta\sigma(2\pi)^{1/2}} \exp \frac{-[\ln(\sigma/\sigma_M)]^2}{2\beta^2} \tag{2.45}$$

where σ_M is the median radar cross section, and β is the standard deviation of $\ln(\sigma/\sigma_M)$.

With regard to the log-normal PDF, it is easy to show that the relations between the average, the most probable, and the median value of σ are simple functions of β:

$$\frac{\bar{\sigma}}{\sigma_M} = \exp \frac{\beta^2}{2} \tag{2.46}$$

and

$$\frac{\sigma_0}{\sigma_M} = \exp \frac{-\beta^2}{2} \tag{2.47}$$

We have by no means exhausted the discussion of different PDFs for the enormous variety of fluctuating radar targets. Such PDFs as Γ, K, Rician are also used. Describing the target statistics faithfully becomes very important when techniques of automatic threshold adjustment are used, which are called constant false-alarm rate (CFAR). Chapter 12 covers this important concept.

The discussion on fluctuating targets referred to complex targets, as well as ground and sea returns, which were termed clutter. Only the statistical qualitites of clutter were discussed. Chapter 4, dedicated to clutter, will cover other concepts that affect the average σ of clutter, such as incident angle, type of illumination, polarity, type of terrain, and roughness.

REFERENCES

2.1 J. W. Crispin and K. M. Siegel, *Methods of Radar Cross-Section Analysis*, Academic Press, New York, 1968.

2.2 Allan E. Fuhs, *Radar Cross Section Lectures*, Department of Aeronautics, Naval Post Graduate School, Monterey, California, 1982.

2.3 Ray J. King, *Micorwave Homodyne Systems*, Peter Peregrinus, Herts., England, 1978.

2.4 R. F. Harrington, "Small Resonant Scatterers and Their Use for Field Measurements," *IRE Trans. Microwave Theory and Techniques*, **MTT-10** (1962), pp. 165–174.

2.5 R. F. Harrington and J. R. Mautz, "Straight Wires with Arbitrary Excitation and Loading," *IEEE Trans. Antennas and Propagation*, **AP-15** (1967), pp. 502–515.

2.6 Athanasios Papoulis, *Probability, Random Variables, and Stochastic Processes*, 2nd ed., McGraw-Hill, New York, 1984.

2.7 Peter Beckman and Andre Spizzichino, *The Scattering of Electromagnetic Waves from Rough Surfaces*, Pergamon Press, Oxford, 1963, ch. 7.

2.8 M. Sekine, T. Musha, Y. Tomota, T. Hagisawa, T. Irabu, and E. Kiuchi, "Weibull-Distributed Sea Clutter," *IEE Proc. (London) Part F*, **130** (1983), p. 476.

PROBLEMS

2.1 Two metal spheres, one with radius a and the other with radius $2a$, act as a target for a radar at wavelength λ ($a > \lambda$). The spheres are spaced more than several wavelengths apart. The total radar cross section of the two spheres σ is changing with aspect angle. Find the ratio $\sigma_{MAX}/\sigma_{MIN}$. (Ignore shadowing effects.)

2.2 Draw an arbitrary wavefront (perpendicular to the propagating rays) in front of a cut of a corner reflector (Fig. 2.2), and prove that the total path length between the two crossings of that wavefront by any ray is a constant equal to twice the shortest distance between the wavefront and the vertex of the corner reflector.

2.3 Show that the effective area of a dihedral corner reflector is

$$A_{EFF} = 2ab \sin \alpha, \qquad 0 \leq \alpha \leq 45°$$

where a and b are as defined in Fig. 2.3a.

2.4 What will be the angular spacing between the incident and reflected rays if the corner of a dihedral reflector has an angle of $90° + \beta$?

2.5 What is the angle of symmetry of a trihedral corner reflector?

2.6 Show that the average, mean-square, and median values of the Rayleigh PDF (for amplitude) are

$$\bar{A} = A_0(\pi/2)^{1/2}, \quad \overline{A^2} = 2A_0^2, \quad A_M = A_0(\ln 4)^{1/2}$$

2.7 Find the average, mean-square, and median values of $p_5(A)$ (dominant + Rayleigh).

2.8 The median σ is easier to measure than the average σ, because it does not require linear receivers. (The median is the value that is exceeded half the time.) Find the ratio $\bar{\sigma}/\sigma_M$ for a Rayleigh distribution.